Electronic Supplementary Material (ESI) for Journal of Materials Chemistry A

This journal is © The Royal Society of Chemistry 2017

Supporting Information for

Facile fabrication of CuO microcube@Fe-Co_3O_4 nanosheet array as a high-performance electrocatalyst for oxygen evolution reaction

Xiumin Li,[a] Chuncheng Li,[b,c] Akihiro Yoshida, [a,b] Xiaogang Hao,[c] Zhijun Zuo, [c] Zhongde Wang, [c] Abuliti Abudula, [a] and Guoqing Guan[a,b,]*

[a]*Graduate School of Science and Technology, Hirosaki University, 1-Bunkyocho, Hirosaki 036-8560, Japan.*

[b]*North Japan Research Institute for Sustainable Energy (NJRISE), Hirosaki University, Matsubara, Aomori 030-0813, Japan. E-mail: guan@hirosaki-u.ac.jp; Fax: +81-17-735-5411*

[c]*Department of Chemical Engineering, Taiyuan University of Technology, Taiyuan 030024, China.*

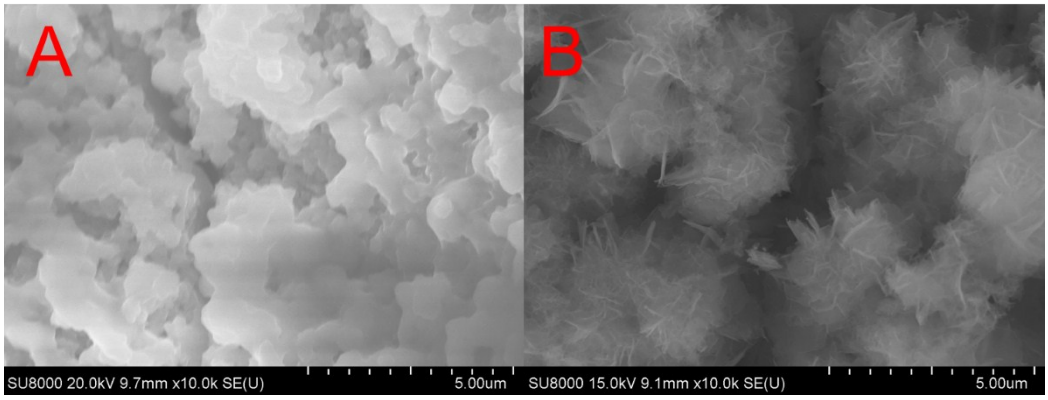

Fig. S1 SEM images of electrodeposited $Fe(OH)_3$ (A) and $Fe(OH)_2$ (B) materials

The $Fe(OH)_3$ material was deposited on a pretreated carbon rod by UPED with an initial solution containing 0.05 M $Fe(NO_3)_3$, while $Fe(OH)_2$ was obtained in 0.05 M $NaNO_3$ and 0.05 $FeSO_4$ solution. The applied potential during the on-time operation was -1.0 V (vs Ag/AgCl). Pulse durations of on-time and off-time were fixed at 1.0 s while pulse repetition time was 500.

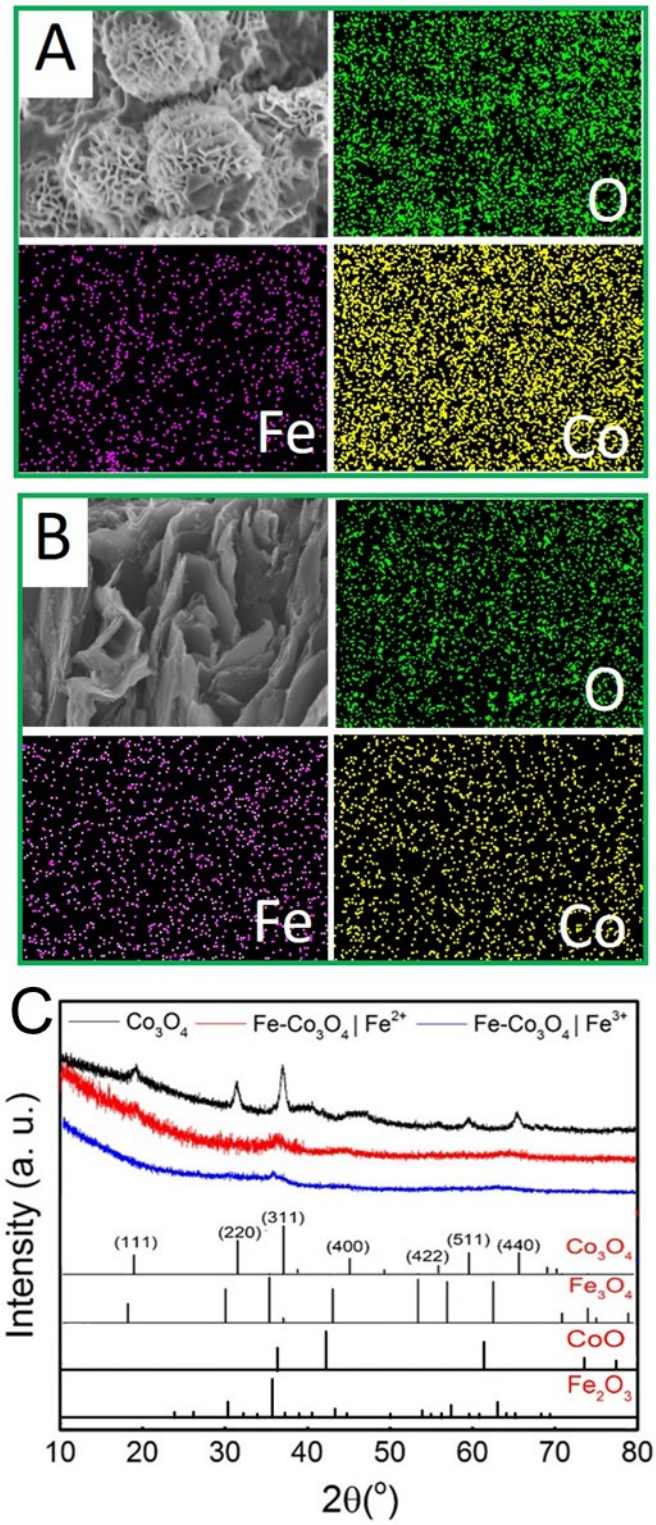

Fig. S2 EDS elemental mapping spectra of Fe-Co_3O_4 | Fe^{2+} material (A), and Fe-Co_3O_4 | Fe^{3+} material (B), and corresponding SEM images. (C) XRD patterns of Co_3O_4 and Fe-Co_3O_4 catalysts.

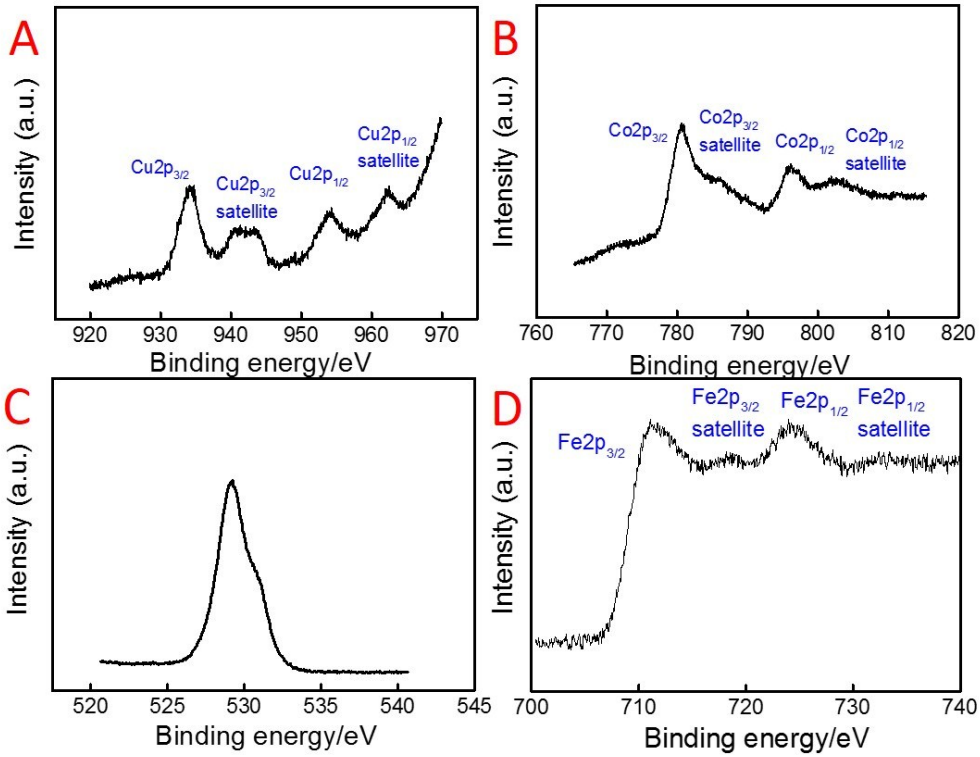

Fig. S3 (A) XPS spectra of CuO/ Fe-Co_3O_4 composite for Cu (A), Co (B), O (C) and Fe (D) elements.

Fig.S3 shows XPS spectra of O, Fe, Cu, and Co elements in CuO/Fe-Co_3O_4 composite. The peaks at around 934, 942, 954, and 962 eV related to the Cu $2p_{3/2}$ and Cu $2p_{1/2}$ spectra, and corresponding satellites while the peaks located at 781, 786, 792 and 803 eV in Fig.S3 reflected the $Co2p_{3/2}$ and $Co2p_{1/2}$ spectra, and corresponding satellites. Fig. S3 C presents the O1s core level spectra where the peaks at 529.2 and 531 eV corresponded to O elements in the Co_3O_4 material and absorbed OH- species, respectively. In addition, the existence of Fe element in Fig. S3 further indicated that it was well incorporated into CuO/Fe-Co_3O_4 composite.

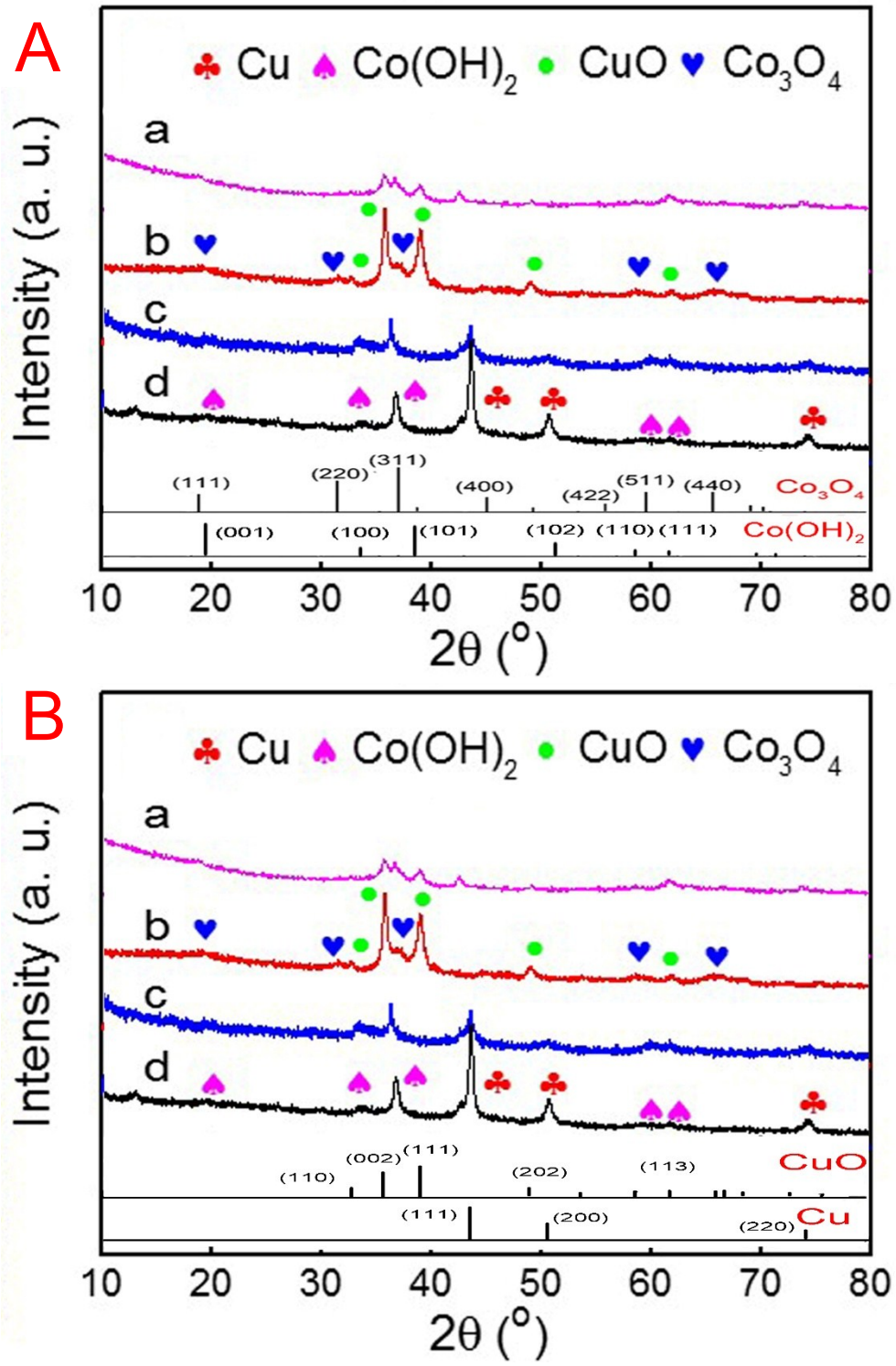

Fig. S4 XRD patterns of CuO/Co_3O_4 and $CuO/ Fe\text{-}Co_3O_4$ composites before and after calcination, a: $CuO/Fe\text{-}Co_3O_4$, b: CuO/Co_3O_4, c: $Cu/Fe\text{-}Co(OH)_2$, d: $Cu/Co(OH)_2$.

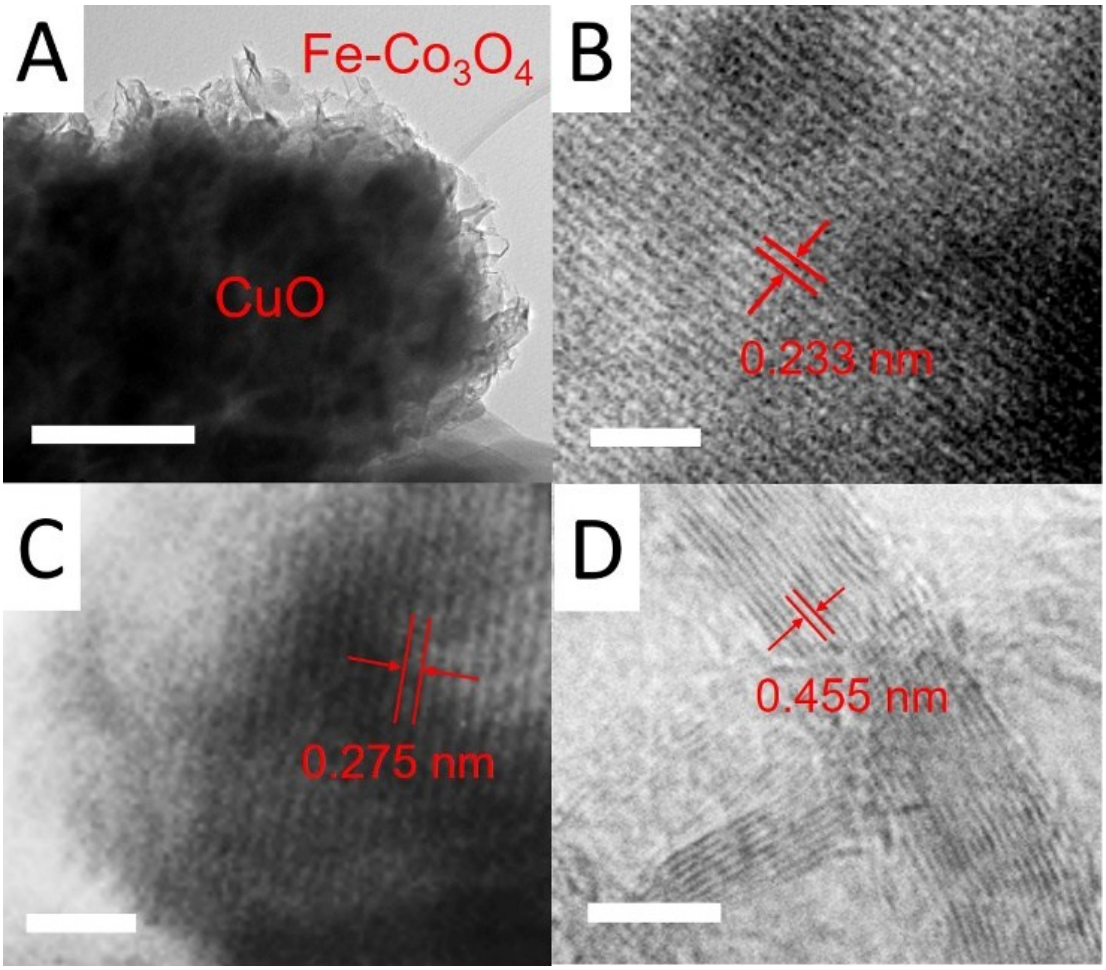

Fig. S5 TEM images of CuO/Fe-Co_3O_4 composite with core-shell structure. Whole particle (A), CuO particle core (B), and Fe-Co_3O_4 nanosheet shell (C, D). Scan bar in A: 500 nm, (B, C): 2 nm, D: 5 nm.

The composite catalyst obtained at -1.0 V was consisted of CuO particle as core and Fe-Co_3O_4 nanosheets as shell. The main reason for the formation of CuO/Fe-Co_3O_4 composite with such hierarchical core/shell arrays should be attributed to the faster reaction rate of Cu^{2+} reduction than Fe-$Co(OH)_2$ deposition. That is, Cu nuclei could be formed at first, and then grow as Cu particle and served as the core during the electrodeposition process of Cu/Fe-$Co(OH)_2$ precursor. Generally, the charge applied on the substrate will concentrate on the embossment parts with higher curvature on the formed core material [1, 2]. Thus, higher potential on the formed Cu particle should be generated during the following deposition process. As a result, Fe-$Co(OH)_2$ nanosheets become easier to be deposited around the Cu particle at higher potential, which will

hinder the lateral growth of Cu particle at the same time. Consequently, with the deposition proceeding, Fe-$Co(OH)_2$ nanosheets were gradually formed on the Cu particle as the shell and finally the hierarchical core/shell structure is obtained.

Table S1. Comparison of electrocatalytic OER activities of intercalated NiFe LDH electrodes with various state-of-the-art OER catalysts.

Catalysts	Electrolyte	η (mV)@ 10 mA cm^{-2}	Ref.
CuO/Fe-Co_3O_4	1M KOH	232	This work
Noble metal-based			
IrO_2/C	0.1M KOH	470	3
IrO_2	0.1M KOH	450	4
Ir/C	1M KOH	300	5
LDH-based			
NiFe LDH /CNT	1M KOH	~235	5
NiFe LDH;	1M KOH	300;	6
NiCo LDH;	1M KOH	330;	6
CoCo LDH	1M KOH	350	6
NiFe LDH;	1M KOH	224	7
NiFe LDH/RGO	1M KOH	245	8
$Ni_{2/3}Fe_{1/3}$-GO	1M KOH	230	9
NiFe LDH /CQDs	1M KOH	~235	10
$FeNi_8Co_2$ LDH	1M KOH	220	11
CoMn LDH	1M KOH	324	12
Transition metal oxides			
Co_3O_4	1M KOH	~270	13
$NiCo_2O_4$	1M KOH	340	14
$Co_3V_2O_8$	0.1M KOH	350	15
CoMoO4	1M KOH	312	16
$CuCo_2O_4$/NrGO	1M KOH	360	17
Other catalysts			
Ni_2P	1M KOH	310	18
Co_4N/CC	1M KOH	257	19
CoP	1M KOH	360	20
CoS/Ti	1M KOH	361	21

Calculation of Electrochemical surface area (ECSA):

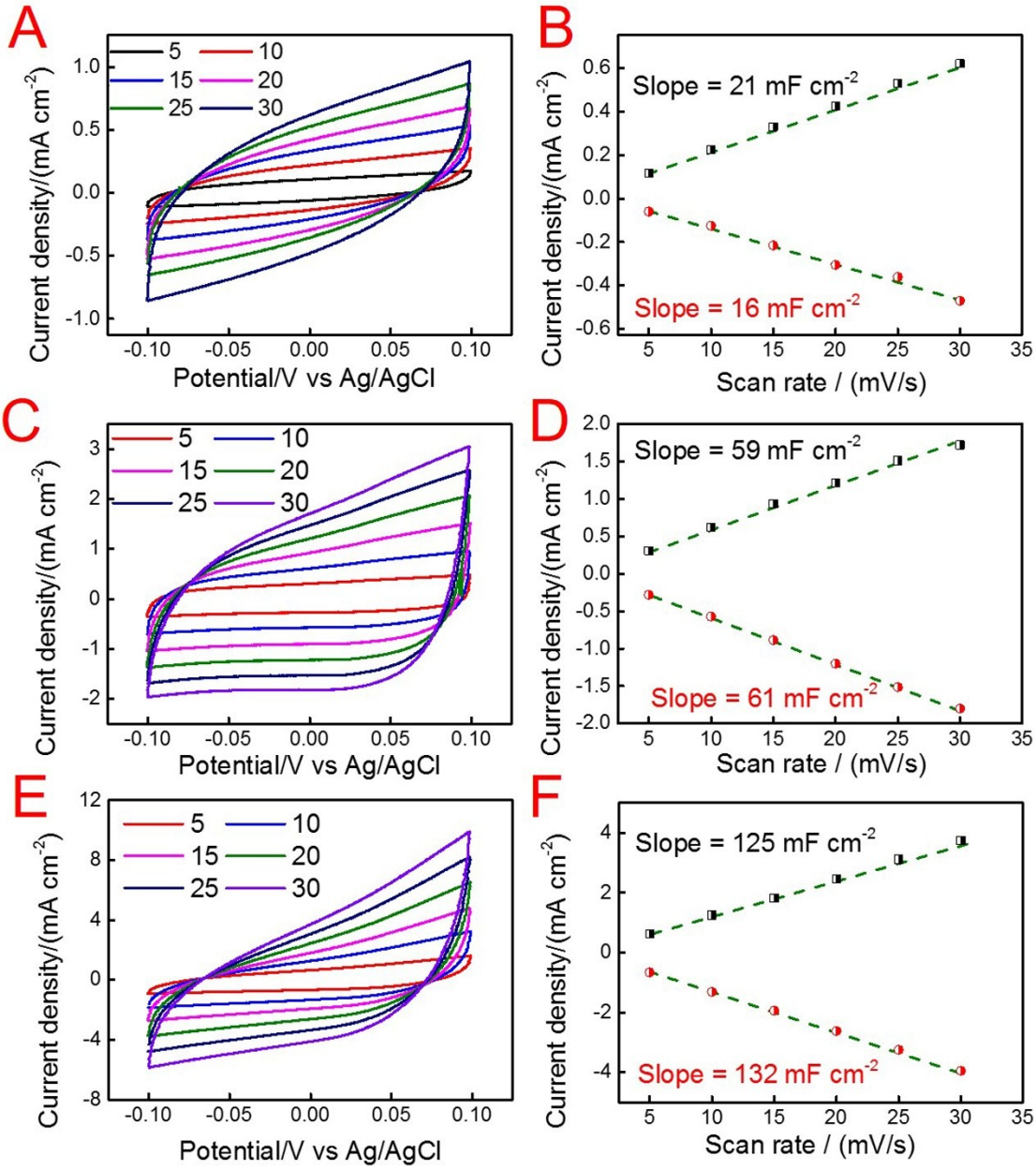

Fig. S6. CVs of pure CuO (A), Fe-Co_3O_4 (C) and CuO/Fe-Co_3O_4 composite (E) between the potential region 0.1 V to -0.1 V (vs Ag/AgCl) with scan rates of 5, 10, 15, 20, 25, and 30 mV/s in KOH solution. The cathodic (○) and anodic (□) charging currents measured at 0 V vs Ag/AgCl plotted as a function of scan rate. The determined double-layer capacitance of the system was taken as the average of the absolute values of the slope after the linear fitting of the data.

The electrochemical active surface areas of the CuO/Fe-Co_3O_4 composite and the corresponding pure CuO and Fe-Co_3O_4 catalysts were evaluated by using the electrochemical double-layer (C_{dl}) capacitance. The amount of the electrical capacitance between the double layers can be measured from the CV curves at different scan rates by the equation

$\nu \times C_{DL} = J_c$

where ν is the scan rate and J_c is the double layer charging current.

The slope obtained from the plot between the double layers charging current and scan rate is directly considered as the double layer capacitance (C_{DL}) of the catalyst.

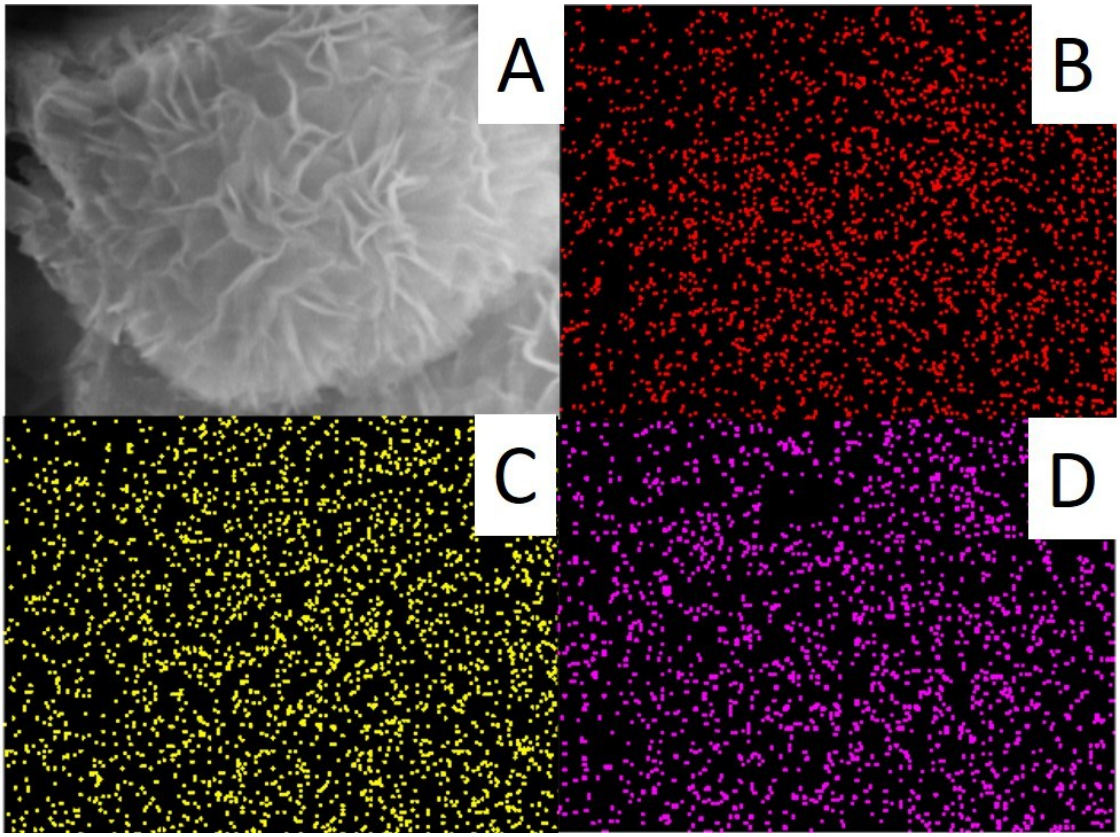

Fig. S7 EDS elemental mapping spectra of CuO/Fe-Co_3O_4 material for (B) Cu, (C) Co, and (D) Fe elements.

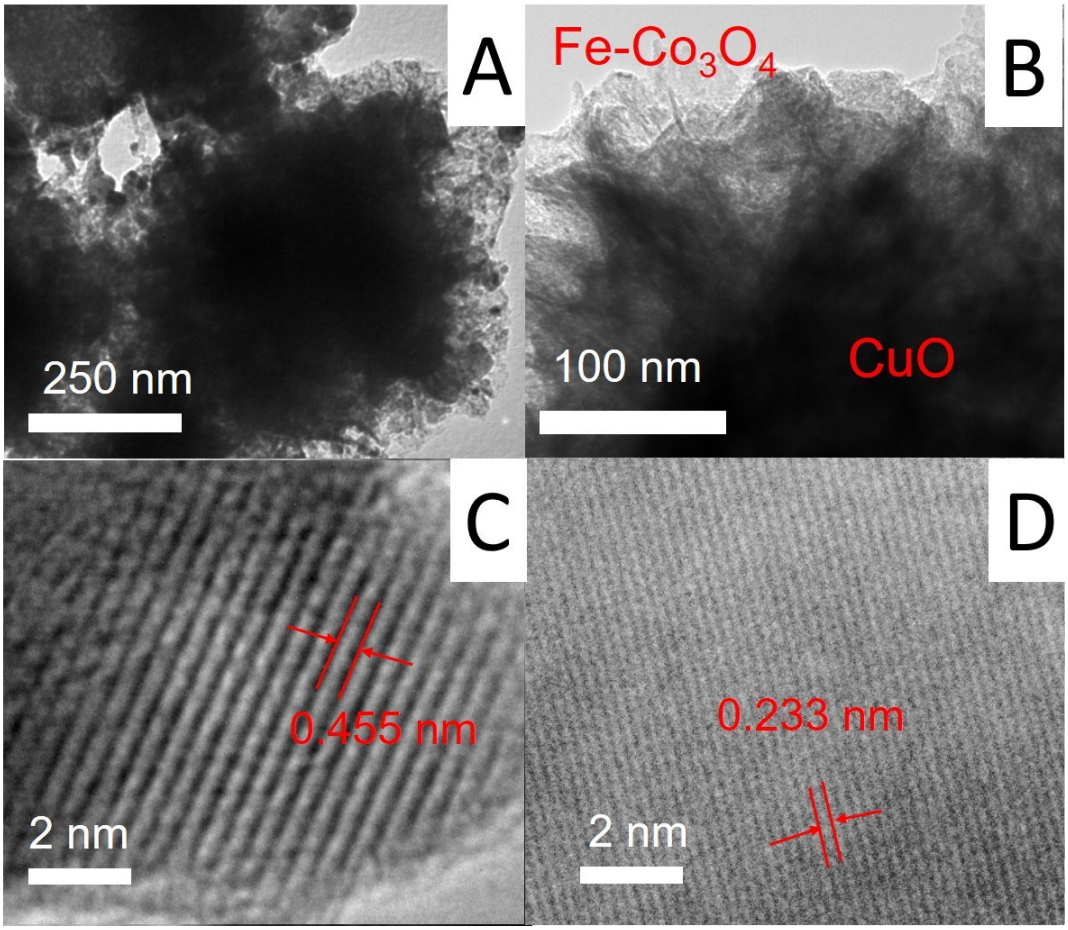

Fig. S8 TEM images of CuO/Fe-Co_3O_4 composite with core-shell array. Whole particle (A, B), Fe-Co_3O_4 nanosheet shell (C), and CuO particle core (D).

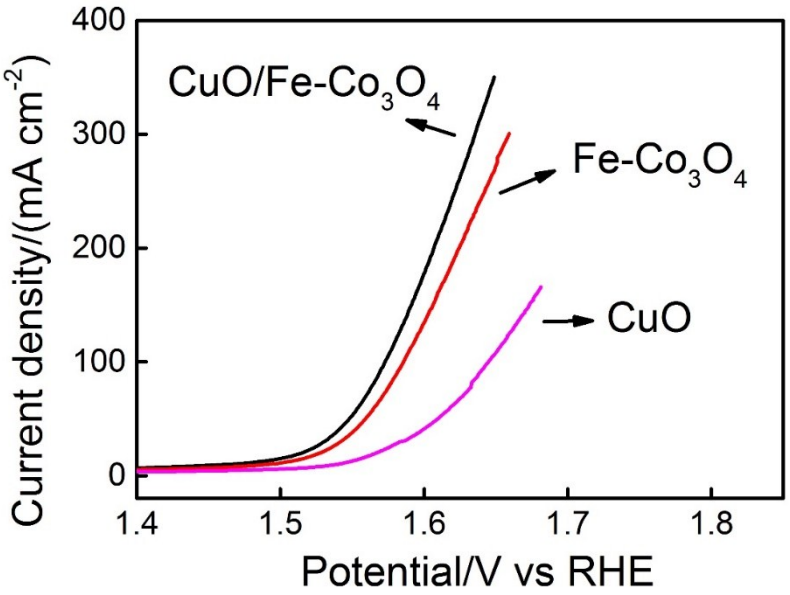

Fig. S9 IR-corrected polarization curves of CuO, Fe- Co_3O_4, and CuO/Fe-Co_3O_4 electrodes.

Reference

1. Brian S. Elliott, 2015, Corona discharge and high voltage leaks, http://library.automationdirect.com/corona-discharge-and-high-voltage-leaks-issue-12-2008/
2. H S Fricker, Why does charge concentrate on points, Phys. Educ. 24 (1989) 157–161.
3. T. Y. Ma, J. L. Cao, M. Jaroniec, S. Z. Qiao, Interacting carbon nitride and titanium carbide nanosheets for high-performance oxygen evolution, Angew. Chem. Int. Ed. 55 (2016) 1138-1142.
4. Y. Zhu, W. Zhou, Z. G. Chen, Y. Chen, C. Su, M. O. Tadé, Z. Shao, $SrNb_{0.1}Co_{0.7}Fe_{0.2}O_{3-\delta}$ Perovskite as a next-generation electrocatalyst for oxygen evolution in alkaline solution, Angew. Chem. Int. Ed. 54 (2015) 3897–3901.
5. M. Gong, Y. Li, H. Wang, Y. Liang, J. Z. Wu, J. Zhou, J. Wang, T. Regier, F. Wei, H. Dai, An advanced Ni–Fe layered double hydroxide electrocatalyst for water oxidation, J. Am. Chem. Soc. 135 (2013) 8452-8455.
6. F. Song. X. Hu, Exfoliation of layered double hydroxides for enhanced oxygen evolution catalysis, Nat. Commun. 5 (2014) Article number: 4477
7. Z. H. Li, M. F. Shao, H. L. An, Z. X. Wang, S. M. Xu, M. Wei, D. G. Evansa, X. Duan, Fast electrosynthesis of Fe-containing layered double hydroxide arrays toward highly efficient electrocatalytic oxidation reactions, Chem. Sci. 6 (2015) 6624-6631.
8. D. H. Youn, Y. B. Park, J. Y. Kim, G. Magesh, Y. J. Jang, J. S. Lee, One-pot synthesis of NiFe layered double hydroxide/reduced graphene oxide composite as an efficient electrocatalyst for electrochemical and photoelectrochemical water oxidation, J. Power Sources 294 (2015) 437-443.
9. W. Ma, R. Ma, C. X. Wang, J. B. Liang, X. H. Liu, K. H. Zhou, T. Sasak, A superlattice of alternately stacked Ni–Fe hydroxide nanosheets and graphene for efficient splitting of water, ACS Nano 9 (2015) 1977–1984.

10. D. Tang, J. Liu, X. Y. Wu, R. H. Liu, X. Han, Y. Z. Han, H. Huang, Y. Liu, Z. H. Kang, Carbon quantum dot/NiFe layered double-hydroxide composite as a highly efficient electrocatalyst for water oxidation, ACS Appl. Mater. Interfaces 6 (2014) 7918–7925.
11. X. Long, S. Xiao, Z. L. Wang, X. L. Zheng, S. H. Yang, Co intake mediated formation of ultrathin nanosheets of transition metal LDH—an advanced electrocatalyst for oxygen evolution reaction, Chem. Commun. 51 (2015) 1120-1123.
12. F. Song, X. L. Hu, Ultrathin cobalt–manganese layered double hydroxide is an efficient oxygen evolution catalyst, J. Am. Chem. Soc. 136(2014)16481–16484.
13. R. C. Li, D. Zhou, J. X. Luo, W. M. Xu, J. W. Li, S. S. Li, P. P. Cheng, D. S. Yuan, The urchin-like sphere arrays Co_3O_4 as a bifunctional catalyst for hydrogen evolution reaction and oxygen evolution reaction, J. Power Sources 341 (2017) 250–256.
14. X. M. Lv, Y. H. Zhu, H. L. Jiang, X. L. Yang, Y. Y. Liu, Y. H. Su, J. F. Huang, Y. F.Yao, C. Z. Li, Hollow mesoporous $NiCo_2O_4$ nanocages as efficient electrocatalysts for oxygen evolution reaction, Dalton Trans. 44 (2015) 4148-4154.
15. S. Hyun, V. Ahilan, H. Kim, S. Shanmugam, The influence of $Co_3V_2O_8$ morphology on the oxygen evolution reaction activity and stability, Electrochem. Commun. 63 (2016) 44–47.
16. M. Q. Yu, L. X. Jiang, H. G. Yang, Ultrathin nanosheets constructed $CoMoO_4$ porous flowers with high activity for electrocatalytic oxygen evolution, Chem. Commun. 51(2015)14361-14364.
17. S. K. Bikkarolla, P. Papakonstantinou, $CuCo_2O_4$ nanoparticles on nitrogenated graphene as highly efficient oxygen evolution catalyst, J. Power Sources 281 (2015) 243-251.
18. A. L. Han, H. L. Chen, Z. J. Sun, J. Xua P. W. Du, High catalytic activity for water oxidation based on nanostructured nickel phosphide precursors, Chem. Commun. 51 (2015) 11626-11629.

19. P. Chen, K. Xu, Z. Fang, Y. Tong, J. Wu, X. Lu, X. Peng, H. Ding, C. Wu, Y. Xie, Metallic Co_4N porous nanowire arrays activated by surface oxidation as electrocatalysts for the oxygen evolution reaction, Angew. Chem. 127 (2015) 14923–14927.
20. J. Ryu, N. Jung, J. H. Jang, H. J. Kim, S. J. Yoo, In situ transformation of hydrogen-evolving CoP nanoparticles: toward efficient oxygen evolution catalysts bearing dispersed morphologies with Co-oxo/hydroxo molecular units, ACS Catal. 5 (2015) 4066–4074.
21. T. T. Liu, Y. H. Liang, Q. Liu, X. P. Sun, Y. Q. He, A. M. Asiri, Electrodeposition of cobalt-sulfide nanosheets film as an efficient electrocatalyst for oxygen evolution reaction, Electrochem. Commun. 60 (2015) 92–96.